

Phase diagram of solution of oppositely charged polyelectrolytes

Rui Zhang and B. I. Shklovskii

Theoretical Physics Institute, University of Minnesota, Minneapolis, Minnesota 55455

(Dated: October 7, 2018)

Abstract

We study a solution of long polyanions (PA) with shorter polycations (PC) and focus on the role of Coulomb interaction. A good example is solutions of DNA and PC which are widely studied for gene therapy. In the solution, each PA attracts many PCs to form a complex. When the ratio of total charges of PA and PC in the solution, x , equals to 1, complexes are neutral and they condense in a macroscopic drop. When x is far away from 1, complexes are strongly charged. The Coulomb repulsion is large and free complexes are stable. As x approaches to 1, PCs attached to PA disproportionate themselves in two competing ways. One way is inter-complex disproportionation, in which PCs make some complexes neutral and therefore condensed in a macroscopic drop while other complexes become even stronger charged and stay free. The other way is intra-complex disproportionation, in which PCs make one end of a complex neutral and condensed in a small droplet while the rest of the complex forms a strongly charged tail. Thus each complex becomes a “tadpole”. These two ways can also combine together to give even lower free energy. We get a phase diagram of PA-PC solution in a plane of x and inverse screening radius of the monovalent salt, which includes phases or phase coexistence with both kinds of disproportionation.

PACS numbers: 61.25.Hq, 82.35.Rs, 87.14.Gg, 87.15.Nn

I. INTRODUCTION

Condensation in solution of two oppositely charged polyelectrolytes (PE) is an important phenomenon in biology and chemical engineering. One of the most interesting applications is DNA condensation by polycations (PC), which is widely used in gene therapy research. A good example is condensation of DNA with poly-lysine [1]. Complexation of DNA with PCs can invert the charge of bare DNA and help DNA to penetrate negatively charged cell membrane. At the same time, adsorbed PC in complexes or their condensate may protect DNA from digestion by enzymes inside the cell [2]. Tremendous amount of experimental works have been done in this area [1, 2, 3, 4, 5, 6, 7].

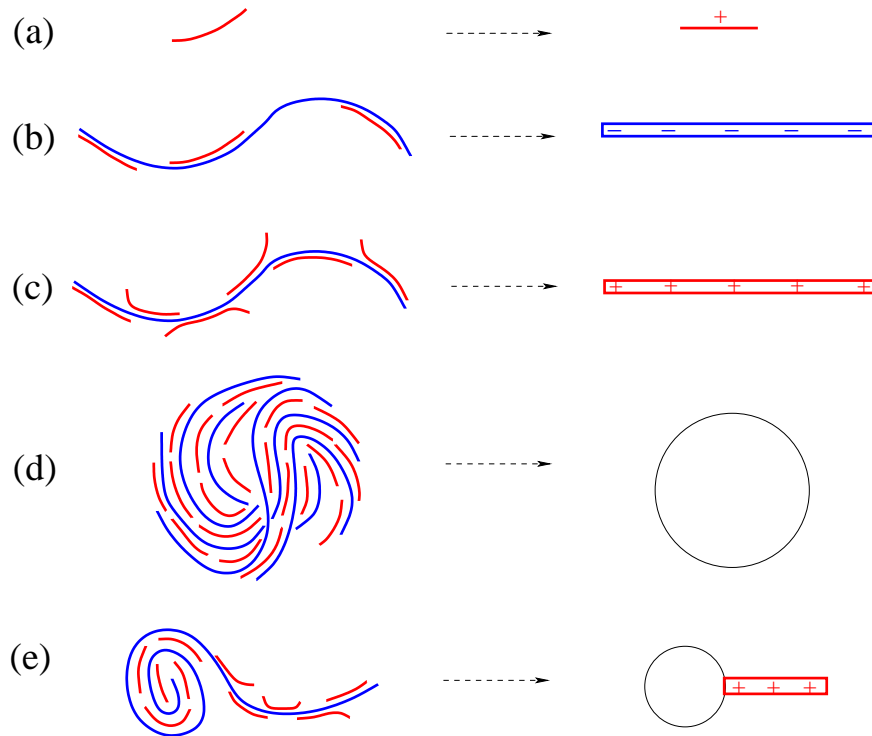


FIG. 1: Objects appearing in a solution of PA and PC (left column) and their symbols used in Figs. 2, 4, 9 and 10 (right column). The long polymer is PA and the short polymer is PC. (a) a single PC. (b) negative PA-PCs complex. (c) positive PA-PCs complex. (d) condensate of almost neutral complexes. (e) tadpole made of one PA-PCs complex. Here only the case of positive tail is shown. The tail can be negative, too.

In this paper, motivated by DNA-PC condensation, we study the equilibrium state of a solution of polyanions (PA) and polycations (PC) in the presence of monovalent salt and

focus on the role of Coulomb interaction. We assume that both PA and PC are so long that at room temperature T their translational entropy can be ignored in comparison with their Coulomb energy. We are particularly interested in the case when PA is much longer than PC and many PCs are needed to neutralize one PA. In Fig. 1 we list objects which can appear in such a solution. Each PA attracts many PCs to form a PA-PCs complex (Fig. 1b,c). Neutral complexes can further condense in a liquid drop (Fig. 1d). One complex can form a neutral head and a charged tail to become a tadpole (Fig. 1e). And it is possible to have excessive free PCs (Fig. 1a). When and where these objects exist or co-exist with each other depends on two dimensionless parameters: the ratio of total charges of PC and PA in the solution, x , and b/r_s , where b is the size of the monomer and r_s is the Debye-Hückel screening radius provided by monovalent salt. The main result of this paper is the phase diagram in a plane of x and b/r_s as shown in Fig. 2. We discover a new phase of “tadpoles” originating from the polymer nature of the objects. We also present a first theory of broadening of the phase of a single drop with decreasing r_s (curves $x_4(r_s)$ and $x'_4(r_s)$ in Fig. 2).

Up to now, there was no complete theory of phase diagram for such systems. Previously, the complexation of oppositely charged polyelectrolytes was studied in a symmetric system in which the length, concentration and linear charge density of PA and PC are the same [8, 9]. It was shown that even in the absence of monovalent salt, strongly charged PA and PC form a single macroscopic drop of neutral dense liquid, which separates from water. It corresponds to the phase at $x = 1$ in our phase diagram (Fig. 2). On the other hand, the phase diagram of a solution of DNA and short polyamines was studied in Refs. [10, 11, 12] in which translational entropy of polyamines plays a very important role. We postpone discussion of the role of translational entropy till the end of this paper (Sec. VI). In our previous works [13, 14], phase diagrams have been discussed for other systems. In Ref. [13], solution of very long PA with positive spheres was considered. This system is similar to chromatin in the sense that each PA binds many spheres making a long necklace. We also discussed the phase diagram of a system of oppositely charged spheres in strongly asymmetric case when each say negative sphere complexes with many positive ones [14]. Many features of the phase diagram in Fig. 2 are also applicable to these systems and we will return to them in the conclusion.

A recent paper of us studied the exactly same topic [15]. But it missed two phase coexistence regions at $r_s \rightarrow \infty$ (comparing Fig. 2 of Ref. [15] with Fig. 2 in this paper). The

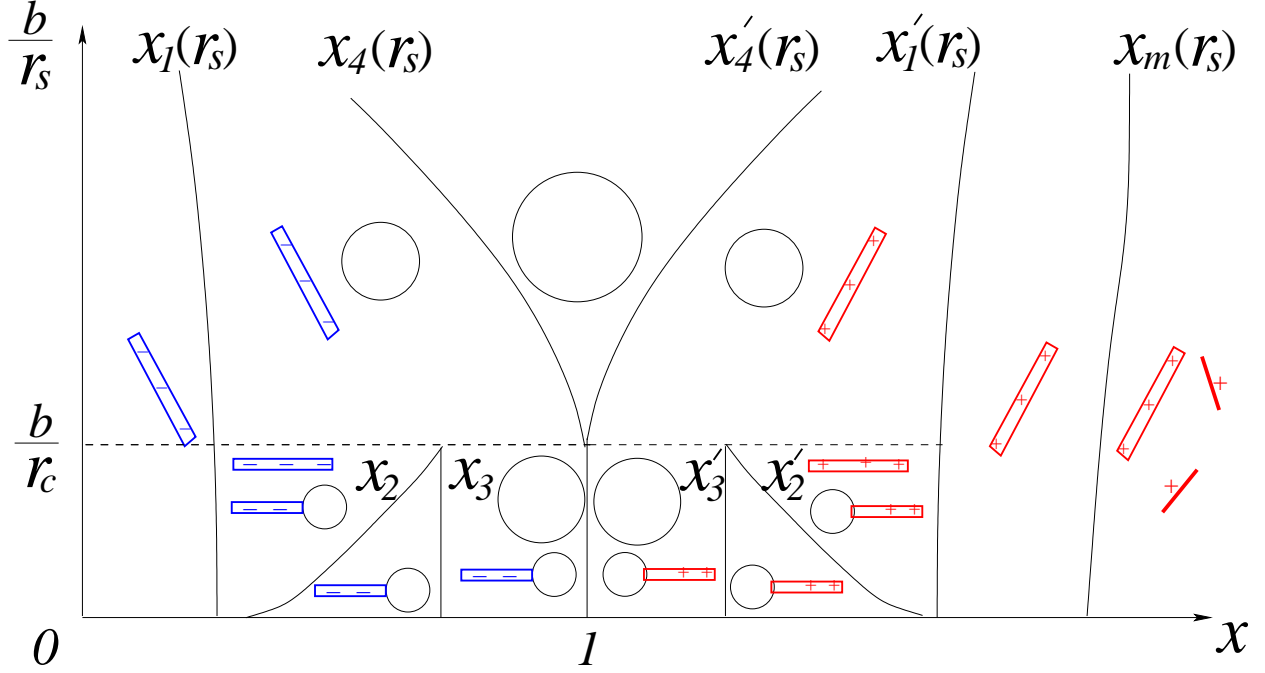


FIG. 2: Typical phase diagram of a solution of PA and PC. The horizontal axis x is the ratio of total charges of PC and PA in the solution. The vertical axis b/r_s is the ratio of the length of a monomer size of the PA molecule to the Debye-Hückel screening radius r_s . Symbols are explained in Fig. 1.

main purpose of the present paper is to make corrections and to discuss the complete phase diagram we have right now.

It is enough to look at $x < 1$ side of Fig. 2 to see the main feature of the phase diagram. It contains three phases: the phase of a single drop for $x > x_4$, the phase of free complexes for $x < x_1$, and the “tadpole” phase for $x_2 < x < x_3$. Between these phases, there are three regions of phase coexistence. This phase diagram is very much similar to the phase diagram of water in temperature and volume coordinates [16], when r_s/b is considered as temperature and x as volume. The three phases mentioned above are like gas, solid and liquid respectively. Essentially, this analogy originates from the Gibbs’ phase rule [16], which is crucial to determine our phase diagram (see Sec. III).

Let us now try to understand the physics of this phase diagram. We start from the horizontal axis ($r_s \rightarrow \infty$) and first focus on $x < 1$ side. In the solution, each PA adsorbs many PCs to form a complex. When $x \ll 1$, the number of PC is not enough to neutralize

all PAs and each PA-PCs complex is strongly negatively charged (Fig. 1b). The Coulomb repulsion between complexes is huge and all complexes stay free, or in other words, colloidal solution of complexes is stable (see ranges $0 < x < x_1$ in Fig. 2).

When $x = 1$, each PA-PCs complex is neutral and there is no Coulomb repulsion between them. They all condense to form a macroscopic strong correlated liquid drop (see Fig. 2). Due to the orderly arrangement of positive and negative charges in the drop, a certain amount of short-range correlation energy is gained (Fig. 3). We define $\varepsilon < 0$ as the energy gain of a neutral complex in the macroscopic drop. Note that monomers on the surface of the drop can not gain as much energy as monomers inside. This defines the surface energy of the drop which plays an important role in the competition between two kinds of disproportionations (see the next paragraph).

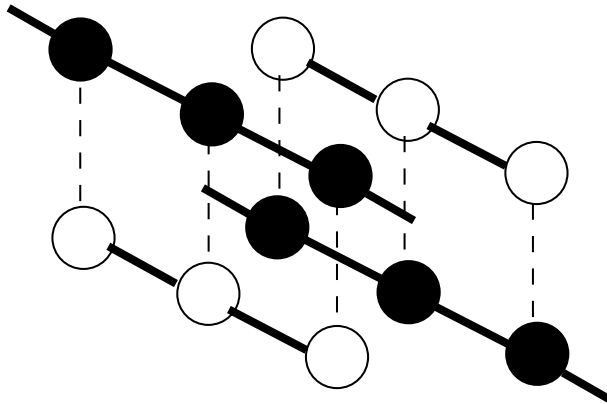


FIG. 3: A schematic illustration of short-range attraction between neutral complexes in a condensed liquid drop using the model of strongly charged PA and PC. A portion of two complexes in the liquid drop is shown. PA and PC charges are shown by black and white dots correspondingly. The dashed lines show two complexes sitting in parallel planes. The complexes attract each other because charges of the same sign are farther away than charges of the opposite sign.

In vicinity of $x = 1$, the long-range Coulomb repulsion between charged complexes competes with the short-range attraction due to correlations. As x increases, condensation starts at $x = x_1$. To minimize the free energy, PCs can be redistributed among complexes so that a portion of complexes are neutral and therefore condensed in a macroscopic drop, while the rest of complexes become stronger charged and stay free. This is called *inter-complex disproportionation* [2] or partial condensation [13] (see Fig. 4a). It is essentially a coexis-

tence of the two phases: the single drop phase and the free complexes phase. On the other hand, PCs can also disproportionate themselves within each complex, which we call *intra-complex disproportionation* (Fig. 4b). PCs move closer to one end of PA molecule, making one part of a PA molecule neutral and condensed in a droplet, while the other part is even stronger charged and not condensed. Unlike inter-complex disproportionation, this gives a new “tadpole” phase, as far as L is finite, where L is the length of a free PA-PCs complex (see Fig. 2). It is possible to combine the two ways of disproportionation to accomplish even lower free energies (see Fig. 4c,d). As a result, at $r_s \rightarrow \infty$, we have the sequence of these phases as shown on the horizontal axis of Fig. 2.

What happens at $x > 1$ side is almost the same, except that here the number of PC is larger than necessary to neutralize all PAs and each complex is strongly positively charged (charge inverted) (Fig. 1c). Let us briefly remind the nontrivial mechanism of charge inversion at $x > 1$ side [17]. We illustrate it in Fig. 5 for the model of strongly charged flexible PA and PC, in which the distance between charges, b , is the same for PA and PC molecules and is of the order of Bjerrum length $l_B = 7\text{\AA}$ ($e^2/Dl_B = k_B T$, $D = 80$ is the dielectric constant of water). When a new PC molecule arrives at a neutral PA-PCs complex, all PCs in the complex can rearrange themselves so that the charge of this excessive PC is smeared in the whole complex and the Coulomb self-energy of the PC is effectively reduced to zero (Fig. 5). This elimination of the Coulomb self-energy is essentially due to correlation of PCs in the complex and can not be described by Poisson-Boltzmann mean field approximation. We define $\mu_c < 0$ (c stands for “correlation”) as the chemical potential related to the elimination of the Coulomb self-energy of PC in the complex. Related to the charge of PC, it acts as an external voltage overcharging PA. With increasing x , the inverted charge of the complex increases. At certain critical $x = x_m$ (m stands for “maximum charge inversion”) (see Fig. 2), the maximum charge inversion is achieved where μ_c is balanced by the Coulomb repulsive energy of the complex to a PC. The topological structure of the phase diagram is almost symmetric about $x = 1$. The only asymmetry appears at $x > x_m$. Here additional PCs are not attracted to maximum charge-inverted PAs and stay free in the solution (see Fig. 2).

Now let us discuss screening by a monovalent salt. This screening effectively cuts off the range of the Coulomb interaction at the distance r_s . As r_s decreases, first the long-range Coulomb repulsion is reduced, while the short-range correlation induced attraction is not

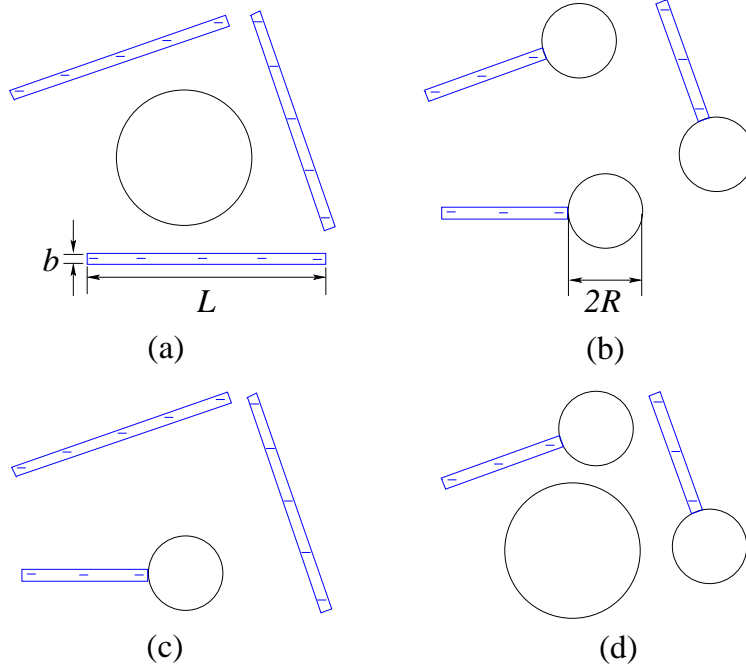


FIG. 4: Possible phases and phase coexistence due to disproportionation. Symbols used here are explained in Fig. 1. (a) Coexistence of free complexes and a single drop (inter-complex disproportionation): PCs disproportionate themselves among PAs so that a portion of PA-PCs complexes are neutral and condensed in a macroscopic drop, while the rest of them are stronger charged and free. (b) The tadpole phase (intra-complex disproportionation): PCs disproportionate themselves within each PA-PCs complex to form a “tadpole”, with a neutral condensed “head” and a charged “tail”. (c) Coexistence of tadpoles and free complexes. (d) Coexistence of tadpoles and a single drop. In these two cases, inter and intra disproportionation are combined to achieve a lower free energy.

affected. Accordingly, all the ranges of condensation in the phase diagram become wider (Fig. 2). Eventually, in the limit of very small r_s , the short-range correlational attraction is also screened out and the macroscopic drop completely dissolves (not shown in Fig. 2). In the intermediate range of r_s we are interested in, there are two major effects of screening. First, the tadpole configuration disappears at certain r_s (Fig. 2). Indeed, if we compare intra and inter disproportionation, the former has a lower Coulomb energy but a higher surface energy. At large r_s , the Coulomb energy is more important and tadpoles are preferred, and vice versa. In the analogy to the phase diagram of water, it is like the solid-vapor phase transition at

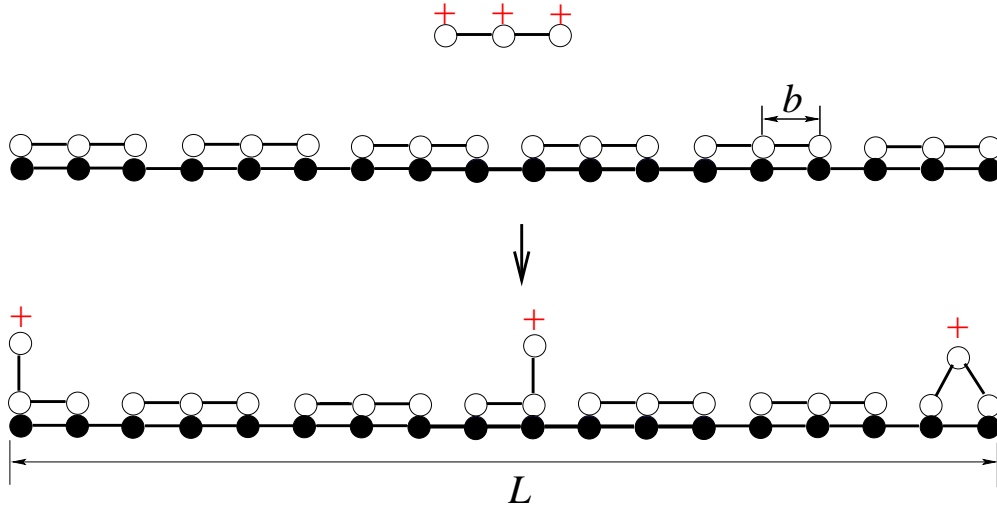


FIG. 5: An illustration of charge inversion of a PA molecule by flexible PCs when they are both strongly charged. Negative PA charges are shown by black dots. Positive PC charges are shown by white dots. When a new PC molecule is adsorbed to a neutral PA-PCs complex, its charge is fractionalized in mono-charges and its Coulomb self-energy is eliminated by redistribution of all PCs in the complex. In reality, the numbers of charges of PA and PC can be much larger than numbers shown here. Imagine for example that PA and PC have charges $-1000e$ and $+100e$.

low temperature. Second, the single drop phase occupies a finite range of x around $x = 1$ at a finite r_s , which grows with $1/r_s^2$ (Fig. 2). Recall that at $r_s \rightarrow \infty$, the macroscopic drop should be neutral and therefore it exists only at $x = 1$. If each condensed complex were charged ($x \neq 1$), the total charge of the macroscopic drop would be proportional to its volume and the Coulomb energy per unit volume would be huge proportional to its surface. On the other hand, at r_s much smaller than the size of the macroscopic drop, the Coulomb energy is not accumulative but additive for each volume of the size r_s . Therefore the macroscopic drop can tolerate some charge density and the range of the single drop phase in the phase diagram widens.

Currently our theory can be compared with experiments only qualitatively since in many cases it is not clear, whether the equilibrium state of the system is reached in experimental times due to the slow kinetics. Also the interesting tadpole phase could be very hard to realize due to a very large critical r_s above which tadpoles can exist. In solutions of DNA with PC, charge inversion of complexes is observed at $x > 1$ [1, 2]. The size of condensed

particles reaches maximum close to $x = 1$ corresponding to the single drop phase in our phase diagram. When $x \neq 1$, the size of condensed particles decreases in agreement with our equilibrium phase diagram [1, 2, 3]. In solutions of DNA with basic polypeptides, at $x < 1$, it is observed that DNA molecules exist simultaneously in two distinct conformations, i.e., elongated conformation and condensed conformation [4]. This corresponds to a phase coexistence of free complexes and a single drop in our phase diagram ($x_1 < x < 1$ in Fig. 2). On the other hand, the enhancement of condensation with the help of simple salt is observed in Ref. [1]. Certain tadpole-like phases have also been observed in experiments [1, 5, 6], although we do not think they are equilibrium tadpole phases discussed in this paper.

This paper is organized as follows. In Sec. II, we discuss all possible phases when $r_s \rightarrow \infty$. We then consider the role of screening by monovalent salt and get the complete phase diagram in Sec. III. In Sec. IV, we discuss $x > 1$ side more carefully and reveal another possibility for the phase diagram. In Sec. V, we estimate parameters ε and μ_c microscopically in the case of strongly charged PA and PC. In Sec. VI, we discuss the role of translational entropy of PC in connection with previous works [13, 14]. We conclude in Sec. VII.

II. PHASES IN THE ABSENCE OF MONOVALENT SALT

In this section we discuss all possible phases in the absence of monovalent salt, i.e., $r_s \rightarrow \infty$. Although this situation is not realistic, it serves as a start point for more complicated theory at finite r_s (see Sec. III). Here and below, We focus on the role of the Coulomb interaction and neglect all other interactions such as hydrophobic force. We focus on $x < 1$ side and postpone the discussion of $x > 1$ side till Sec. IV.

Let us first clarify the terminology “phase”. By definition, a phase of a system containing one or several substances is an equilibrium homogeneous state [16]. The chemical potential of each substance in each phase is uniquely defined and calculated independently. In the present case, we have a system of two substances: PA and PC. Following the definition, there are three possible phases: the phase of a single drop (Fig. 1d), the phase of free complexes (Fig. 1b), and the tadpole phase (Fig. 2e). Although we cannot proof rigidly that only these three phases can appear in the phase diagram, we have a quite convincing argument. We show in the last subsection of this section that three possible phases or phase coexistence are ruled out by free energy considerations.

At $x = 1$, there is no Coulomb repulsion between complexes, the phase of a single drop is preferred due to the short range correlation energy gain (see Fig. 3). At $x \ll 1$, the phase of free complexes is preferred because of strong Coulomb repulsion between complexes. Then it is natural to conclude that the tadpole phase, which is kind of combination of the other two phases, appears in vicinity of $x = 1$. To testify this idea, we focus on possible phase coexistent regions. For example, the phase of free complexes can coexist with the tadpole phase, and the tadpole phase can coexist with the phase of a single drop. By minimizing the free energies in these two regions respectively, we can find the ranges of x in which one or the other phase is preferred, or the two phases coexist. This leads to the phase diagram at $r_s \rightarrow \infty$.

A. The free energies of the three phases

For pedagogical reason, let us start from the free energy of the tree phases. We first notice that the Coulomb energy of each charged complex can be calculated by considering it as a conductor with certain capacitance. To see this, let us recall that the total chemical potential of a PC molecule adsorbed in PA is given by

$$\mu = \mu_c + q\phi. \quad (1)$$

Here the first term is the correlational chemical potential, and the second term is the electric energy of a PC given by the local electric potential ϕ in the complex. Since both μ and μ_c are the same along the complex, ϕ must be the same in the complex. It is in this sense that the PA-PCs complex can be considered as a conductor and the concept of capacitance can be used to calculate its Coulomb energy.

We denote N as the total number of PA molecules in the solution. For the phase of free complexes (see Fig. 1b), we have

$$F = N \left[\frac{(nq - Q)^2}{2C} + nE(n) \right]. \quad (2)$$

Here C is the capacitance of a free complex, $-Q$ and q are the bare charges of PA and PC, n is the number of PC in each free PA-PCs complex, and $E(n) < 0$ is the correlation energy of a PC in a complex as a function of n . In this expression, the first term is the Coulomb self-energy of free complexes. The second term is the negative correlation energy of PCs

in free complexes. We emphasize again that we study very long and strongly charged PC and PA such that their translational entropies are negligible. Since all PCs are adsorbed to PAs, the net charge of each free complex, $(nq - Q)$, is equal to $(x - 1)Q$. We will show in Sec. V that near the phase coexistence region, $|n - n_i| \ll n_i$, where $n_i = Q/q$ is the number of PC in a neutral complex. Consequently, $\mu_c(n) = \partial[nE(n)]/\partial n$ is approximately equal to its value μ_c at $n = n_i$. Furthermore, it is convenient to consider the average free energy of each complex, $f = F/N$, instead of F . Finally, we rewrite the free energy as

$$f = \frac{(x - 1)^2 Q^2}{2C} + \frac{(x - 1)Q}{q} \mu_c + n_i E(n_i), \quad (3)$$

where C is given by

$$C = \frac{DL}{2 \ln(L/b)} \quad (4)$$

as the capacitance of a cylindrical capacitor. Here L is the length of a free PA-PC complex and $D = 80$ is the dielectric constant of water.

Using similar notations, for a phase of a single drop (see Fig. 1d), we have

$$f = n_i E(n_i) + \varepsilon. \quad (5)$$

Here remember that each complex in the drop is neutral. The expression includes the negative correlation energy of PCs in neutral complexes, and the negative correlation energy of a neutral complex due to condensation, ε .

For a tadpole phase (see Fig. 1e), we denote z as the fraction of the tail part of each complex. We have

$$f(z) = \frac{(x - 1)^2 Q^2}{2C_t} + (1 - z)\varepsilon \left(1 - \frac{3b}{R}\right) + \frac{(x - 1)Q}{q} \mu_c + n_i E(n_i). \quad (6)$$

This free energy is almost a combination of the last two free energies except two differences. First, the capacitance of a tadpole is determined by its tail, given by

$$C_t = \frac{DzL}{2 \ln(zL/b)}. \quad (7)$$

Second, the correlation energy due to condensation is gained only in the ‘‘head’’ of the tadpole. Therefore there is an additional factor $1 - z$ in the second term. The surface energy of the head is also included in the second term [18]. R is the radius of the head of the tadpole (see Fig. 4b), given by

$$R = \left[\frac{3}{16} (1 - z) b^2 L \right]^{1/3}. \quad (8)$$

B. The phase diagram at $r_s \rightarrow \infty$

Now we are ready to discuss the free energy in the phase coexistence regions and get the phase diagram at $r_s \rightarrow \infty$. We first consider the coexistence of the phase of free complexes and the tadpole phase (see Fig. 4c). We denote y as the fraction of tadpoles in the coexistence. Combining Eqs. (3) and (6), we have

$$f(y, z) = \frac{(x-1)^2 Q^2}{2[yC_t + (1-y)C]} + y(1-z)\varepsilon \left(1 - \frac{3b}{R}\right) + \frac{(x-1)Q}{q} \mu_c + n_i E(n_i). \quad (9)$$

Here the first term is the Coulomb energy of the system of free complexes and tadpoles with capacitances C and C_t correspondingly. These capacitances are additive because all complexes are in equilibrium with respect of exchange of PC and the electric potential of all complexes is the same (see discussion at the beginning of the subsection II A).

To Minimize this free energy with respect of two variables y and z , it is convenient to separate the free energies into two parts

$$f(y, z)/|\varepsilon| = \left[\alpha \frac{(1-x)^2 \ln(L/b)}{1-y+yz} - y(1-z) \right] + \left[\alpha \frac{(1-x)^2 yz \ln z}{(1-y+yz)^2} + \frac{5y(1-z)^{2/3}}{(L/b)^{1/3}} \right], \quad (10)$$

where

$$\alpha = \frac{Q^2}{DL|\varepsilon|} \quad (11)$$

is in order of 1 for strongly charged PA and PC (see Sec. V), and Eqs. (4), (7) and (8) have been used. In this expression, the last two terms of Eq. (9) have been neglected since they are independent of y, z . The first square bracket contains the main terms of the Coulomb energy and the correlation energy, in which $\ln zL$ in C_t has been replaced by $\ln L$ and the surface energy has been ignored. The second square bracket contains correction terms in the first order to make up the two neglects in the main terms. We will see below that the small parameter we used to expand this free energy is $\ln(L/b)/(L/b)^{1/3}$, for $L \gg b$.

We first minimize the main terms in Eq. (10) and get

$$y(1-z) = 1 - (1-x)\sqrt{\alpha \ln(L/b)}. \quad (12)$$

Putting it back to the correction terms in Eq. (10) and taking the minimum, we get

$$z = 1 - \left[\frac{5 \ln(L/b)}{3(L/b)^{1/3}} \right]^{3/4}. \quad (13)$$

Combining the above two conditions, we have

$$y = \left[1 - (1-x)\sqrt{\alpha \ln(L/b)} \right] \left[\frac{3(L/b)^{1/3}}{5 \ln(L/b)} \right]^{3/4}. \quad (14)$$

Specifically, considering $y = 0$ and $y = 1$, we get the boundaries of the phase coexistent region (see Fig. 2)

$$1 - x_1(\infty) = \frac{1}{\sqrt{\alpha \ln(L/b)}}, \quad (15)$$

$$1 - x_2(\infty) = \frac{1}{\sqrt{\alpha \ln(L/b)}} \left\{ 1 - \left[\frac{5 \ln(L/b)}{3(L/b)^{1/3}} \right]^{3/4} \right\}. \quad (16)$$

Here and below $x(\infty)$ means $x(r_s \rightarrow \infty)$. When x increases from $x_1(\infty)$ to $x_2(\infty)$, y increases from 0 to 1 linearly. This is actually the level rule [16] and the sign of a first order phase transition.

For a very long PA, $L \gg b$, parameter $\ln(L/b)/(L/b)^{1/3} \ll 1$. Therefore z is close to 1, the free energy expansion in Eq(10) is self-consistent. Also $x_1(\infty)$ is close to 1 and $x_2(\infty)$ is close to $x_1(\infty)$.

We consider the other phase coexistent region (see Fig. 4d) following the same approach. Combining Eqs. (5) and (6), we have

$$f(y, z) = \frac{(x-1)^2 Q^2}{2yC_t} + y(1-z)\varepsilon \left(1 - \frac{3b}{R} \right) + (1-y)\varepsilon + \frac{(x-1)Q}{q} \mu_c + n_i E(n_i). \quad (17)$$

The free energy similar to Eq. (10) is

$$f(y, z)/|\varepsilon| = \left[\alpha \frac{(1-x)^2 \ln(L/b)}{yz} + yz - 1 \right] + \left[\alpha \frac{(1-x)^2 \ln z}{yz} + \frac{5y(1-z)^{2/3}}{(L/b)^{1/3}} \right]. \quad (18)$$

Minimizing the main terms (in the first square bracket), we get

$$yz = (1-x)\sqrt{\alpha \ln(L/b)}. \quad (19)$$

Putting it back to the correction terms (in the second square bracket) and taking the minimum, we get

$$z = \frac{5 \ln(L/b)}{(L/b)^{1/3}}. \quad (20)$$

Combining the two conditions, we have

$$y = \frac{(1-x)\sqrt{\alpha}(L/b)^{1/3}}{5\sqrt{\ln(L/b)}}. \quad (21)$$

Therefore the boundaries of this coexistent region are (see Fig. 2)

$$1 - x_3(\infty) = \frac{1}{\sqrt{\alpha \ln(L/b)}} \frac{5 \ln(L/b)}{(L/b)^{1/3}}, \quad (22)$$

$$1 - x_4(\infty) = 0. \quad (23)$$

We see that the same small parameter $\ln(L/b)/(L/b)^{1/3}$ works here. Again, the phase transition from the tadpole phase to the phase of a single drop is in the first order.

C. Why not other phases

In this subsection, we argue that several other possible phases or phase coexistence do not appear in the phase diagram at $r_s \rightarrow \infty$.

One possibility would be that the tadpole phase does not appear at all, but the coexistence of the other two phases shows up in vicinity of $x = 1$. This is called inter-complex disproportionation (Fig. 4a). We showed in Ref. [15] that this coexistence has a higher free energy than the tadpole phase in some range of $x < 1$. As far as the tadpole phase exist, it immediately follows that the only phase coexistent regions can exist are those involving tadpoles (see Fig. 4c,d). And the inter-complex disproportionation region (Fig. 4a) has nowhere to show up.

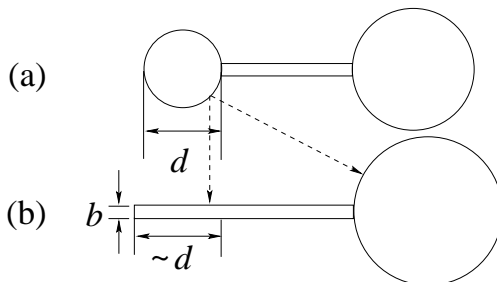


FIG. 6: Comparison of two-heads and one-head configurations. (a): a two-head configuration. The diameter of the smaller head is d . (b): a one-head configuration made from (a) by combining the two heads then releasing tail of length order of d from the head, such that the two configurations have same capacitance. The Coulomb energy is the same for the two configurations, but the surface energy is higher in (a).

The second possibility is a phase in which every complex has more than one “head” and therefore forms a necklace structure. Let us argue that the one-head-one-tail tadpole

configuration is the best for intra-complex disproportionation. To do this, we have to include the capacitances of heads which gives a small correction to Eq. (7). First of all, let us show that for a complex with given charge, one head is better than two heads. Consider an arbitrary two-heads configuration with the diameter of the smaller head d (Fig.6a). We can always construct an one-head configuration from it by combining the two heads then releasing additional tail of the order of d from the head in such a way that the capacitances of the two configurations are the same (Fig.6b). The total free energy consists of the long-range Coulomb energy and the short-range correlation energy in droplets. For the two configurations, the Coulomb energies are the same since the capacitances are equal. But the surface energy is higher in the two-heads configuration since the surface is much larger. Thus, for any two-heads configuration, we can always find a one-head configuration with lower energy. By similar argument, obviously a configuration with many heads along the complex is even worse. Furthermore, the single head always prefers to be at the end of the tail. This can be understood by considering a metallic stick with fixed charge on it. The electric field is larger at the end of the stick than in the middle. Therefore to reduce the Coulomb energy, it is better to put a metallic sphere at the end of the stick to make field there smaller.

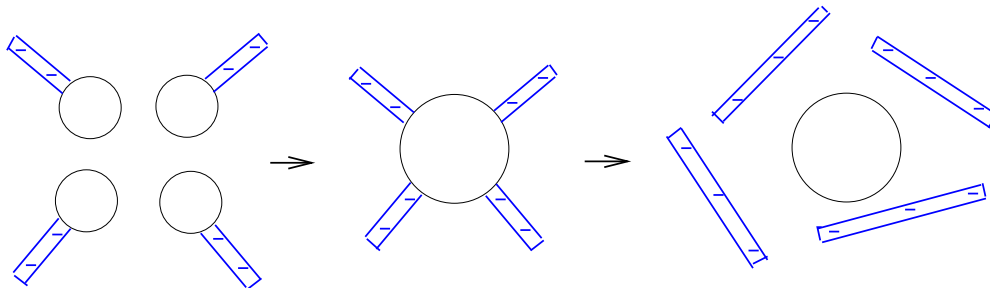


FIG. 7: An illustration of instability of hypothetical micelle-like droplets in a PA-PC system. Symbols are explained in Fig. 1. If tadpoles are not stable, one could think that they merge into micelles. But micelles would immediately break down to reduce Coulomb energy.

The third possibility is a phase in which every few complexes come together to form a micelle-like object (see Fig. 7). However, micelle-like droplets are not stable. For example, suppose several charged PA-PCs tadpoles would gain energy merging into a micelle. Instead of sharing one head by several tails, to reduce the Coulomb energy, it is better to break

the micelle into one tadpole and several tails. Repeating this process, certainly one ends up with a two phase coexistence (see Fig. 7).

Finally, we want to point out that the necklace phase and the micelle phase are always worse in free energies than the tadpole phase. This is not only true at $r_s \rightarrow \infty$. One can show that they do not exist in the case of finite r_s too.

III. PHASE DIAGRAM IN A PLANE OF SCREENING RADIUS AND CHARGE RATIO

In this section, we consider a more realistic situation of finite r_s and get the complete phase diagram in a plane of b/r_s and x (see Fig. 2). Again we focus on $x < 1$ side. The r_s range we are interested in is $b \ll r_s \ll L$. As r_s becomes smaller than L , the long-range Coulomb repulsion is first reduced while the short-range correlational attraction is not affected. Eventually, when $r_s < b$, the short-range correlational attraction is also screened out and the macroscopic drop completely dissolves but we do not consider such salt concentrations. In the range of our interest, $b \ll r_s \ll L$, there are two major implications of screening (see Fig. 2). First, the phase of single drop grows up. Second, the tadpole phase and related phase coexistent regions are destroyed.

Let us first discuss the general confinement to the phase diagram given by the Gibbs' phase rule [16]. Suppose the number of coexistent phases is m . Then for our two substances system, the number of independent equations following the condition of equal chemical potentials is $2(m-1)$. The number of unknowns is $m+1$. For example, they can be chosen as the charge ratio x in each phase and the common parameter b/r_s shared by all coexistent phases. To have a solution to the equations, we require $2(m-1) \leq m+1$. This gives $m \leq 3$. That is to say, the number of coexistent phases cannot be more than 3. It is convenient to define a chemical potential

$$\mu_x = \frac{\partial f}{\partial x}, \quad (24)$$

and consider the phase diagram on a plane of μ_x and b/r_s (see Fig. 8). When three phases coexist, all variables are completely determined. It corresponds to a point in the phase diagram (the triple point). When two phases coexist, there is one thermodynamic degree of freedom. It corresponds to a line in the phase diagram. If we change variable from μ_x to its conjugate variable, x , we get our phase diagram (Fig. 2). One can easily show that in this

phase diagram, three phases coexist on a line, and two phases coexist in a region.

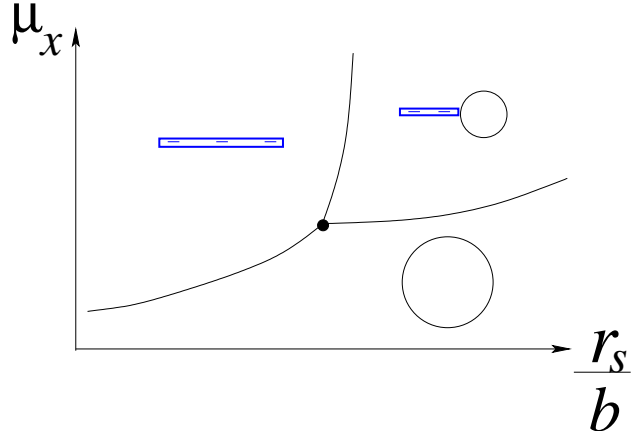


FIG. 8: Schematic phase diagram on a plane of μ_x and r_s . Here μ_x is a chemical potential which is conjugate to x .

The phase diagrams we get is very much similar to the phase diagram of water [16]. Indeed, if we consider μ_x as pressure, r_s/b as temperature, and x as volume, then Fig. 8 is like the PT diagram, and Fig. 2 is like the TV diagram of water. Notice that in our system, real temperature or pressure plays no role. The system is always at room temperature. And the pressure is negligibly small, since in comparison of the Coulomb energy, we have completely ignored the translational entropies of PA and PC, which is related to the volume and the pressure of the system.

Having figured out the topological structure of the phase diagram, let us determine all phase boundaries by considering the three two-phase coexistent regions. We start from the coexistence of tadpoles and free complexes (Fig. 4c). In the presence of monovalent salt, the free energy is still given by Eq. (9), but the expressions of C and C_t can be different. Let us first assume that $zL < r_s \ll L$. Then C_t is still given by Eq. (7), while C is now

$$C = \frac{DL}{2 \ln(r_s/b)}. \quad (25)$$

Following the same procedure as in subsection II B, we get

$$z = \frac{r_s}{2.7L} \exp \left[-\frac{5 \ln(r_s/b)}{3(L/b)^{1/3}} \right], \quad (26)$$

$$y = \frac{1 - (1-x)\sqrt{\alpha \ln(r_s/b)}}{1-z}. \quad (27)$$

At $y = 0$ and $y = 1$, we get the boundaries of this coexistent region (see Fig. 2)

$$1 - x_1(r_s) = \frac{1}{\sqrt{\alpha \ln(r_s/b)}}, \quad (28)$$

$$1 - x_2(r_s) = \frac{r_s}{2.7L\sqrt{\alpha \ln(r_s/b)}} \exp\left[-\frac{5 \ln(r_s/b)}{3(L/b)^{1/3}}\right]. \quad (29)$$

In the limiting case of $r_s \rightarrow L$, these equations go back to Eqs. (15) and (16).

If $r_s \ll zL$, not only C , but also C_t gets a new expression

$$C_t = \frac{DzL}{2 \ln(r_s/b)}. \quad (30)$$

In this case, one can check that the free energy given by Eq. (9) does not have a minimal extremum. Indeed, the Coulomb energy of the system becomes so short-ranged that there is almost no difference to distribute all charges to free complexes or tadpoles. The surface energy of heads dominates and the coexistence of free complexes and the single drop is preferred (see Fig. 2).

We now consider the coexistence of tadpoles with the single drop (Fig. 4d). In the case of finite r_s , the free energy given by Eq. (17) should be revised to

$$f(y, z) = \frac{(x-1)^2 Q^2}{2[yC_t + (1-y)C']} + y(1-z)\varepsilon \left(1 - \frac{3b}{R}\right) + \frac{(x-1)Q}{q} \mu_c + n_i E(n_i). \quad (31)$$

Here C' represents the capacitance of a condensed complex in the single drop. As discussed in Sec. I, when $r_s \rightarrow \infty$, the macroscopic condensate is almost neutral and the phase of single drop exist only at $x = 1$. For finite r_s , the macroscopic drop can tolerate certain charge density. Therefore C' appears. In order to calculate C' , we assume that the macroscopic drop is uniformly charged [19]. If the charge density of the macroscopic drop is ρ and the charge of each complex is $\pi b^2 L \rho / 4$ [18], the electrical potential of the macroscopic drop is

$$\phi = \int_0^\infty \frac{\rho e^{-r/r_s}}{Dr} 4\pi r^2 dr = \frac{4\pi r_s^2 \rho}{D}, \quad (32)$$

This gives

$$C' = \frac{\pi b^2 L \rho}{4\phi} = \frac{Db^2 L}{16r_s^2}. \quad (33)$$

When $r_s \rightarrow \infty$, the capacitance $C' \rightarrow 0$ as expected.

In the case of $zL < r_s \ll L$, C_t is still given by Eq. (7). Minimizing the free energy as in subsection IIB, we get

$$z = \frac{5 \ln(L/b)}{(L/b)^{1/3}} + \frac{\ln^2(L/b)}{8(r_s/b)^2}. \quad (34)$$

And y is still given by Eq. (19). Setting $y = 0$ and $y = 1$, the boundaries of the coexistent region are (see Fig. 2)

$$1 - x_3(r_s) = \frac{1}{\sqrt{\alpha \ln(L/b)}} \frac{5 \ln(L/b)}{(L/b)^{1/3}} \left[1 + \frac{(L/b)^{1/3} \ln(L/b)}{40(r_s/b)^2} \right], \quad (35)$$

$$1 - x_4(r_s) = 0. \quad (36)$$

In the other case of $r_s \ll zL$, C_t is given by Eq. (30). Again the free energy Eq. (31) has no minimal extremum but a maximal extremum. And the minimal free energy is achieved at $z = 1$. This leads to the coexistence of free complexes and the single drop is preferred (see Fig. 2).

We are now ready to determine the position of the line at which three phases coexist in Fig. 2 (it is also the upper boundary of the tadpole phase and the two two-phase coexistent regions). The critical r_s , r_c , is determined by the cross point of $x_2(r_s)$ and $x_3(r_s)$. In the leading order, we have

$$r_c \simeq L^{2/3} b^{1/3} \ln(L/b). \quad (37)$$

Unfortunately, r_c is large and not easily realized in experiments. For example, for $b = 7 \text{ \AA}$ and $L = 100b$, $r_c \simeq 99b = 693 \text{ \AA}$. This means that the tadpole phase and all phase coexistence related with it are typically not relevant to experiments. Physically, comparing with inter-complex disproportionation, the tadpole phase (intra-complex disproportionation) is better in the Coulomb energy, and worse in the surface energy. For the Coulomb energy to be more important, r_s has to be large. Therefore the tadpoles must be extinct at small r_s .

Finally we consider the coexistence of free complexes and the single drop (see Fig. 4a) when $r_s < r_c$. Combining Eqs. (3) and (5), we have

$$f(y) = \frac{(x-1)^2 Q^2}{2[yC + (1-y)C']} + (1-y)\varepsilon + \frac{(x-1)Q}{q} \mu_c + n_i E(n_i), \quad (38)$$

where C is given by Eq. (25). Minimizing the free energy, we have

$$(x-1)^2 \left[\frac{1}{\ln(r_s/b)} - \frac{b^2}{8r_s^2} \right] = \frac{D|\varepsilon|L}{Q^2} \left[\frac{y}{\ln(r_s/b)} + \frac{(1-y)b^2}{8r_s^2} \right]^2. \quad (39)$$

And

$$1 - x_1(r_s < r_c) = \frac{1}{\sqrt{\alpha \ln(r_s/b)}}, \quad (40)$$

$$1 - x_4(r_s < r_c) = \frac{b^2}{8r_s^2} \sqrt{\frac{\ln(r_s/b)}{\alpha}}. \quad (41)$$

Here we put $r_s < r_c$ as the argument to remind us that these expressions are meaningful only at $r_s < r_c$. We see that the width of the single drop phase grows proportionally to $1/r_s^2$ with decreasing r_s (see Fig. 2). When $r_s \rightarrow r_c$, $x_4(r_s) \rightarrow 1$ as expected.

IV. POSSIBLE NEW PHASES AT $x > 1$ SIDE

In this section, we discuss the phase diagram at $x > 1$ side. At $x > 1$, the number of PC molecules is more than enough to neutralize all PA molecules. The signs of charges of free complexes or the tails of tadpoles are inverted to positive. In spite of this difference, all physics we discussed in the last two sections remain valid. Therefore one expects that the topological structure of the phase diagram is symmetric about $x = 1$. And the boundaries $x'_i(r_s)$ (see Fig. 2) satisfy

$$x'_i - 1 = 1 - x_i, \quad (42)$$

where $i = 1, 2, 3, 4$.

However, a little asymmetry exists since the charge inversion process cannot go forever, but reaches its maximum value at certain critical value of x , x_m . x_m is determined from the balance of the gain in the correlation energy with the overall Coulomb repulsive energy for a PC molecule. For example, for a free complex, we have

$$|\mu_c| = \frac{(x_m - 1)Qq}{C}, \quad (43)$$

where each free complex carries net charge $(x_m - 1)Q$. In this equation, the left hand side is the magnitude of the gain in correlation energy, and the right hand side is the Coulomb repulsive energy given by the net charge of the complex. At $x > x_m$, extra PC molecules are not attracted to the complexes, but stay free in solution (see Fig. 2). Using Eq. (25), we get

$$x_m(r_s) = 1 + \frac{DL|\mu_c|}{2Qq \ln(r_s/b)}. \quad (44)$$

When $r_s \rightarrow \infty$,

$$x_m(r_s) = 1 + \frac{DL|\mu_c|}{2Qq \ln(L/b)}. \quad (45)$$

Furthermore, the existence of x_m gives another possibility to the phase diagram. For our purpose, it is enough to consider the simple case where the free complexes and the single drop coexist (see Fig. 4a). One can show that the conclusion is the same for phase coexistence involving tadpoles.

Indeed, what we discussed above is self-consistent if $x'_1 < x_m$. But what if $x'_1 > x_m$? To answer this question, we first notice that x'_1 has another physical meaning. In Eq. (39), for the accuracy we needed, keeping the first term on each side, we get the net charge of each free complex in the phase coexistent region

$$\frac{(x-1)Q}{y} = \frac{Q}{\sqrt{\alpha \ln(r_s/b)}}. \quad (46)$$

According to Eq. (40), this net charge is equal to $(x'_1 - 1)Q$. When $x'_1 > x_m$, to keep the phase coexistence, each free complex should carry charge $(x'_1 - 1)Q$ while it is only allowed to carry $(x_m - 1)Q$ because of the finite correlation chemical potential μ_c . In this situation, x'_1 loses its physical meaning and the charge of each free complex saturates at the maximum value $(x_m - 1)Q$. The free energy of Eq. (38) should be revised to

$$f(y) = y \frac{(x_m - 1)^2 Q^2}{2C} + y \frac{(x_m - 1)Q}{q} \mu_c + (1 - y)\varepsilon + n_i E(n_i). \quad (47)$$

Here for the purpose of discussion, the second order term related to C' has been ignored. With help of Eqs. (40) and (43), this free energy can be written as

$$f(y) = -y \frac{(x_m - 1)^2 Q^2}{2C} - (1 - y) \frac{(x'_1 - 1)^2 Q^2}{2C} + N n_i E(n_i). \quad (48)$$

Clearly, when $x'_1 > x_m$, the minimum of $f(y)$ is reached at $y = 0$. Therefore at $x > 1$ side, we arrive at a phase of total condensation in which all complexes are condensed but some PCs are free. This leads to a different phase diagram (Fig. 9).

It is convenient to classify all PA-PC systems into two categories. In the first category, $x'_1(\infty) < x_m(\infty)$, and we have phase diagram Fig. 2. In the second category, $x'_1(\infty) > x_m(\infty)$, and we have phase diagram Fig. 9. Interestingly, both two categories are realistic as we will see in Sec. V. Notice that in the second case, decreasing r_s to a critical value, r_0 , eventually leads to inversion of inequality $x'_1 > x_m$ (see Fig. 9). We discuss this effect in detail in the next section after we estimate ε and μ_c microscopically.

In the case when $x'_1(\infty) > x_m(\infty)$, the phase of single drop expands around $x = 1$ with growing L/r_s at $x > 1$ side too (see Fig. 9). We calculate the boundary of this phase with the phase of total condensation at $r_s > r_0$. What we need to find out is just how many excessive PCs the macroscopic drop can tolerate at finite r_s . Applying the condition of maximum charge inversion to a condensed complex, similarly to Eq. (43), we have

$$|\mu_c| = \frac{(x'_s - 1)Qq}{C'}. \quad (49)$$

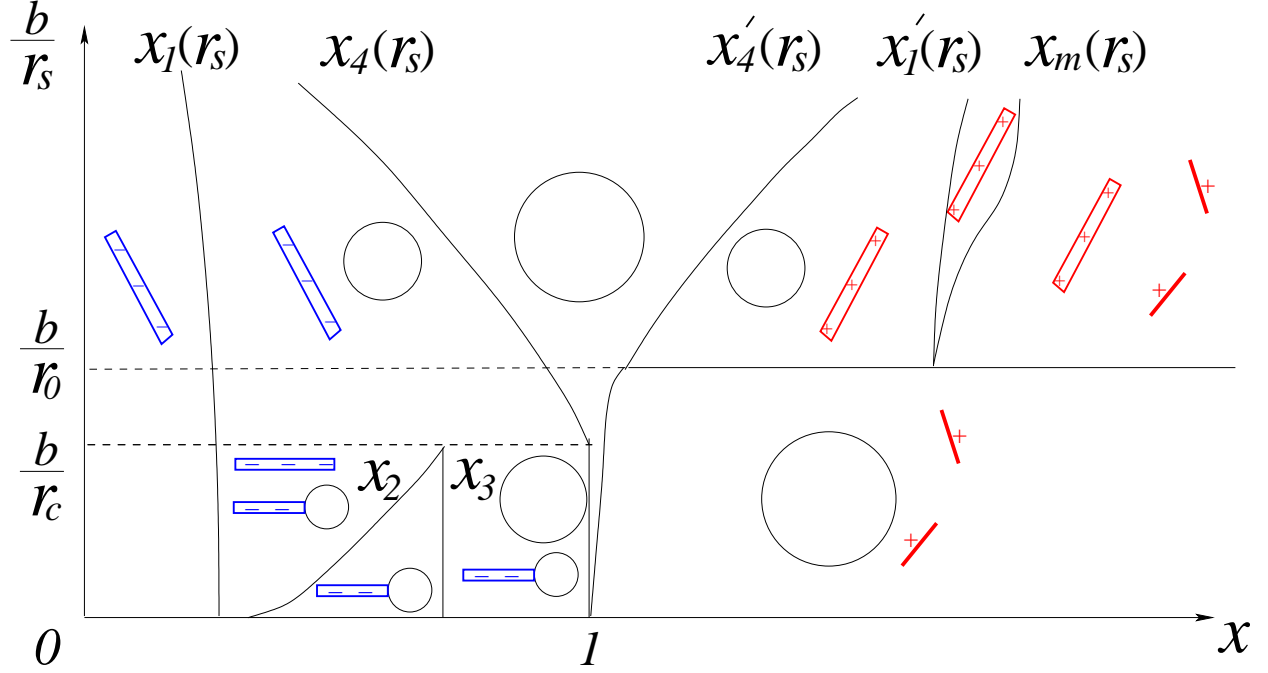


FIG. 9: Phase diagram of solution of PA and PC in the case when at $r_s \rightarrow \infty$, we formally have $x'_1 > x_m$. The meaning of axes and symbols are the same as Fig. 2.

Therefore

$$x'_1(r_s < r_0) = 1 + \frac{D|\mu_c|b^2L}{16Qqr_s^2}. \quad (50)$$

At $r_s < r_0$, we arrive at inequality $x'_1(r_s) < x_m(r_s)$ and Eq. (40) gives the boundary of the phase of single drop (see Fig. 9). We will discuss the transition at $r_s = r_0$ in detail in the next section.

V. PHASE DIAGRAM OF STRONGLY CHARGED POLYELECTROLYTES

In this section, we consider a simple system where linear charge densities of PA's and PC's are equal. Both of them are strongly charged such that every monomer carries a fundamental charge e and $e^2/Db \simeq k_B T$ (see Fig. 5). We estimate parameters ε and μ_c microscopically and choose from the two phase diagrams shown in Figs. 2 and 9.

We first consider the case of $r_s \rightarrow \infty$. As discussed in Sec. I, μ_c is equal to the Coulomb self-energy of a PC,

$$\mu_c = -\frac{qe}{Db} \ln(q/e). \quad (51)$$

On the other hand, when neutral PA-PCs complexes condense, they form a strongly correlated liquid. Monomers of two PEs locally form NaCl-like structure such that the energy in order of $-e^2/Db$ per monomer is gained (Fig. 3) [18]. Therefore

$$\varepsilon \simeq -\frac{Qe}{Db}. \quad (52)$$

We see that indeed α defined by Eq. (11) is in order of 1.

Substituting $L = Qb/e$ into Eqs. (15) and (45), we have

$$x'_1(\infty) \simeq 1 + \frac{1}{\sqrt{\ln(Q/e)}}, \quad (53)$$

$$x_m(\infty) = 1 + \frac{\ln(q/e)}{2\ln(Q/e)}. \quad (54)$$

Accordingly, we get the critical value of q at which $x'_1 = x_m$,

$$q_c = \exp\left(2\sqrt{\ln(Q/e)}\right). \quad (55)$$

When $q > q_c$, or PC is long enough, $x'_1 < x_m$, we have the phase diagram of reentrant condensation (horizontal axis of Fig. 2). When $q < q_c$, or PC is relatively short, $x'_1 > x_m$, we have the asymmetric phase diagram with total condensation at $x > 1$ side (horizontal axis of Fig. 9). The possibility of having two different phase diagrams for different q is related to the interplay of the logarithms in Eqs. (51) and (54). For fixed Q , when q increases, x_m increases but x'_1 is fixed. Therefore we can have either $x_m < x'_1$ or $x_m > x'_1$ by changing q . Notice that q_c is exponentially smaller than Q .

Now let us consider the effect of screening by monovalent salt. We are interested in the case of $r_s \gg b$ when the short-range correlation is not affected yet and ε is fixed. According to Eq. (40),

$$x'_1(r_s) \simeq 1 + \frac{1}{\sqrt{\ln(r_s/b)}}. \quad (56)$$

In order to discuss $x_m(r_s)$, we consider two different cases, $qb/e \ll r_s \ll Qb/e$ and $b \ll r_s \ll qb/e$. When $qb/e \ll r_s \ll Qb/e$, the chemical potential μ_c is still given by Eq. (51). From Eq. (44),

$$x_m(r_s) = 1 + \frac{\ln(q/e)}{2\ln(r_s/b)}. \quad (57)$$

Accordingly, the critical value of q at which $x'_1(r_s) = x_m(r_s)$ is

$$q_c(r_s) = \exp\left[2\sqrt{\ln(r_s/b)}\right]. \quad (58)$$

It decreases with decreasing r_s . Therefore, for a system with $q < q_c(\infty)$, q can be larger than $q_c(r_s)$ at small r_s . Correspondingly, at $x > 1$, for small r_s , the phase of total condensation is replaced by the phase coexistence of free complexes and the single drop. We have a phase diagram shown in Fig. 9. Letting $q = q_c(r_s)$, we get the critical value of r_s at which this phase transition happens

$$r_0 = b \exp\left(\frac{\ln^2(q/e)}{4}\right). \quad (59)$$

Notice that r_0 is much larger than qb/e .

In Fig. 9, $x'_1(r_s) > x_m(r_s)$ at $r_s > r_0$, while $x'_1(r_s) < x_m(r_s)$ at $r_s < r_0$ ($x'_1(r_s)$ curve at $r_s > r_0$ is not shown). By definition of r_0 , the curves $x'_1(r_s)$ and $x_m(r_s)$ merge at $r_s = r_0$. The curve $x'_s(r_s)$ is given by Eq. (50) for $r_s > r_0$ and Eq. (40) for $r_s < r_0$. At $r_s = r_0$, these two expressions are equal to each other. At $x > 1$ side, the solid line at $L/r_s = L/r_0$ corresponds to a first order phase transition. Notice that r_0 can be either smaller or larger than r_c . Here for simplicity, only the former case is shown in Fig. 9.

When $b \ll r_s \ll qb/e$,

$$\mu_c = -\frac{qe}{Db} \ln(r_s/b), \quad (60)$$

and $x_m(r_s) = 3/2$ [17]. In this case, we always have $x'_1(r_s) < x_m(r_s)$ as shown in Figs. 2 and 9.

Finally, in all cases discussed above, the value of x'_1 is close to 1, i.e., $|n - n_i| \ll n_i$ in the condensation regime. Therefore the approximation used in Sec. II that μ_c is a constant is valid.

VI. THE ROLE OF THE TRANSLATIONAL ENTROPY OF POLYCATIONS

A major approximation in this paper is that the translational entropy of PCs is negligible (we can always ignore PA's translational entropy since it is much longer than PC). In this section, we would like to discuss the validity of this approximation and the role of the translational entropy.

First, let us estimate when this approximation is valid. Consider PCs with concentration p in the solution. The free energy due to its translational entropy is $k_B T \ln(pv_0)$, where v_0 is the normalizing volume. On the other hand, according to Eq. (51), the Coulomb energy is in the order of $-qe/Db \simeq -qk_B T/e$. They are equal at the critical value, $p = \exp(-q/e)/v_0$.

Therefore for a long PC with large q , we can ignore PC's translational entropy even at exponentially small p .

If PC is very short, its translational entropy should be included. DNA with short polyamines is a good example of such systems [10, 11, 12]. In this case, the phase diagram gets another dimension, say, the concentration of PC, p . The effect of PC entropy was discussed in detail in Ref. [13, 14] in which the phase diagram is drawn in a plane of two concentrations of oppositely charged colloids at given r_s . Here we discuss the same effect in the language of total charge ratio x used in this paper in the simple case where $x'_1 > x_m$ and $r_s \rightarrow \infty$. For simplicity, we neglect the possibility of intra-molecule disproportionation and the tadpole phase.

In this case, the free energy in Eq. (38) gets an additional term due to the translational entropy of PCs [13]

$$f(n, y) = y \left[\frac{(nq - Q)^2}{2C} + nE(n) \right] + (1 - y)[n_i E(n_i) + \varepsilon] + \left[\frac{xQ}{q} - yn - (1 - y)n_i \right] \ln \left[\left(p - \frac{ynq}{xQ}p - \frac{1 - y}{x}p \right) \frac{v_0}{e} \right], \quad (61)$$

where e is the natural exponential. Here the expression in the square bracket before the logarithm represents the number of free PC in the solution, while the expression in the round bracket in the logarithm represents their concentration.

Now n and y are two independent variables. Taking $\partial F/\partial n = 0$ and $\partial F/\partial y = 0$, we get

$$\mu_c = \ln \left[\left(p - \frac{ynq}{xQ}p - \frac{1 - y}{x}p \right) v_0 \right] - \frac{(nq - Q)q}{C}, \quad (62)$$

$$\varepsilon = \frac{(nq - Q)^2}{2C} + (n - n_i) \left\{ \mu_c - \ln \left[\left(p - \frac{ynq}{xQ}p - \frac{1 - y}{x}p \right) v_0 \right] \right\}. \quad (63)$$

In Eq. (62), eliminating n by Eq. (63), we can calculate the boundaries of the condensation regime by setting $y = 0$ and $y = 1$. For $y = 0$, we get two boundaries of a total condensation phase,

$$p \left(1 - \frac{1}{x} \right) = p_1, \quad (64)$$

$$p \left(1 - \frac{1}{x} \right) = p'_1. \quad (65)$$

For $y = 1$, we get two boundaries of the free complexes phase,

$$p \left(1 - \frac{x_1}{x} \right) = p_1, \quad (66)$$

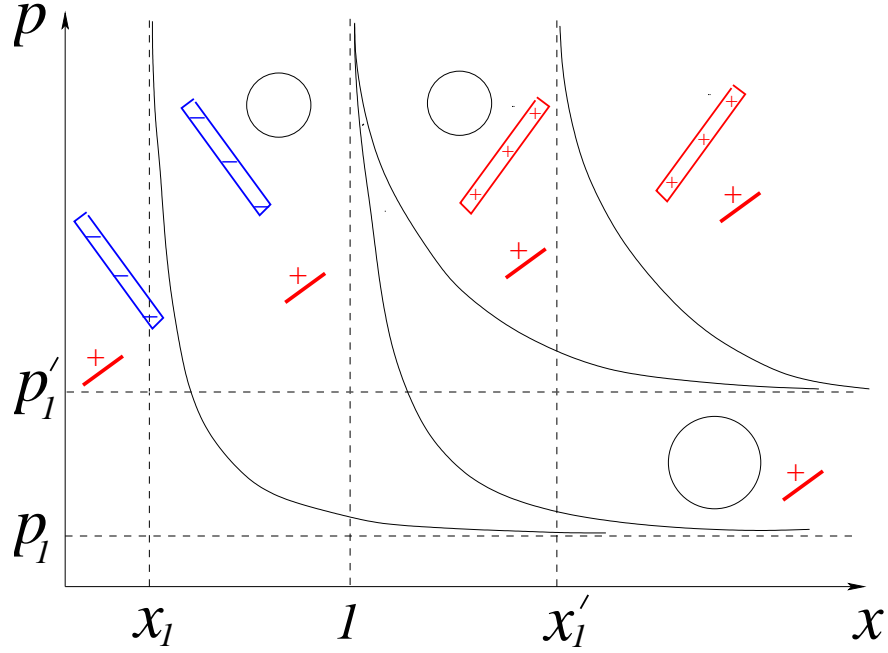


FIG. 10: Phase diagram in a plane of PC's concentration p and total charge ratio x ($x'_1 > x_m$ and $r_s \rightarrow \infty$). Symbols used are explained in Fig. 1. It shows how the phase of total condensation replaces that of partial condensation with decreasing p .

$$p \left(1 - \frac{x'_1}{x} \right) = p'_1. \quad (67)$$

Here

$$p_1 = \frac{1}{v_0} \exp \left(\mu_c - \sqrt{\frac{2|\varepsilon|q^2}{C}} \right), \quad (68)$$

$$p'_1 = \frac{1}{v_0} \exp \left(\mu_c + \sqrt{\frac{2|\varepsilon|q^2}{C}} \right). \quad (69)$$

Accordingly, as shown in the phase diagram Fig. 10, a regime of total condensation is sandwiched by two regimes of partial condensation, which are further sandwiched by two regimes of free complexes.

In Fig. 10, results of previous sections are recovered in the limit $p \rightarrow \infty$. Due to the translational entropy of PC, at finite p all critical x are shifted to higher values. At the same time, a total condensation region acquires a finite width even in the absence of monovalent salt [13]. In the limiting case where $x \rightarrow \infty$, the concentration of PA is much smaller than that of PC, and the entropy of PC is fixed, which offers a fixed charging voltage to PA.

As a result, all PA-PCs complexes are either totally condensed or totally free. The partial condensation regime disappears [13].

VII. CONCLUSION

In this paper, we discussed complexation and condensation of PA with PC in a salty water solution. Using ideas of disproportionation of PCs among complexes and inside complexes (inter- and intra-complex disproportionations) we arrived at the two phase diagrams in a plane of x (ratio of total charges of PC and PA) and L/r_s (ratio of the length of PA, L , and the Debye-Hückel screening radius, r_s) shown in Figs. 2 and 9. In the case of strongly charged PA and PC, we find that both two phase diagrams are possible depending on the relative length of PC to PA. Fig. 2 corresponds to a more generic case of relatively long PC, while Fig. 9 to the case of relatively short one. Our phase diagrams show how total condensation is replaced by the partial one and then by phases of stable complexes when x moves away from $x = 1$.

We discovered two new features of the phase diagrams. First, at large screening radius they include a new phase of tadpoles and corresponding phase coexistence. Second, we found that the phase of the single drop formed at x close to 1 widens with decreasing r_s as $1/r_s^2$.

Although we talked about strongly charged PA and PC one can also consider phase diagram of weakly charged PA and PC and develop a microscopic theory for it. In both cases, the qualitative picture is the same since our discussion of the phase diagram is rather general and independent of the microscopic mechanism of the short-range attraction.

As mentioned in the introduction, the problem we solved in this paper should be considered as an example of a more general problem of the phase diagram of the solution of two oppositely charged colloids. Another important system of this kind is a long PA with many strongly charged positive spheres. When long double helix DNA plays the role of PA, this system is a model for the natural chromatin. Therefore, we call such system artificial chromatin [13]. Our phase diagrams with all new features including tadpoles should be valid for artificial chromatin as well.

There is another class of systems where only some of our predictions are applicable. In the Ref. [14] we considered solution of large negative spheres with positive spheres which

are smaller in both radius and charge. Complexation and condensation of such spheres obey the phase diagrams similar to discussed above. For example, screening by monovalent salt again leads to $1/r_s^2$ expansion of the range of the single drop (total condensation) phase. Another our prediction, the tadpole phase, however, is not applicable to this case, because it is essentially based on the polymer nature of PA.

In a case when the role of PA is played by DNA, one should remember that the double helix DNA is so strongly charged that the effect of the Manning condensation by monovalent counterions must be included [13]. Since DNA complexes with positive macroions (PC, positive spheres or multivalent cations), this Manning condensation can be weaker than free DNA due to counterion releasing. The quantitative description of this effect depends on the geometry of the positive macroions and the microscopic structure of the complex in the system [13]. Generally speaking, this effect leads to the renormalization of the bare charge of PA, Q . In this case, total condensation still happens around $x = 1$ but renormalized charge enters in calculation of x . This means that if on the other hand x is evaluated using the bare charge of DNA, all phase diagrams are centered around a smaller than 1 value of x .

Our phase diagrams deal with equilibrium states of the system. But not all of them can be achieved in experimental time scale due to slow kinetics. Therefore it is not easy to directly compare our theory to experiments. For instance, a phase of many condensed particles with finite size is often found in experiments which does not appear in our phase diagram [1, 2, 3, 7]. We believe that this phase is not a real equilibrium state, but the state frozen kinetically [20, 21]. Thus, kinetics is extremely important for applications and we plan to address it in the future.

Acknowledgments

The authors are grateful to V. Budker, A. Yu. Grosberg, and M. Rubinstein for useful discussions. This work was supported by NSF No. DMR-9985785 and DMI-0210844.

[1] V. Budker, V. Trubetskoy, J. A. Wolff, Condensation of non-stoichiometric DNA/Polycation complexes by divalent cations.

- [2] A.V. Kabanov and V. A. Kabanov, *Bioconjugate Chem.* 6 (1995) 7. And references therein.
- [3] E Lai and J. H. van Zanten, *Biophys. J.* 80 (2001) 864.
- [4] K. Minagawa, Y. Matsuzawa, K. Yoshikawa, M. Matsumoto, M. Doi, *FEBS Letts.* 295 (1991) 67.
- [5] D. D. Dunlap, A. Maggi, M. R. Soria, L. Monaco, *Nucleic Acids Research* 25 (1997) 3095.
- [6] A. A. Zinchenko, V. G. Sergeev, S. Murata, K. Yoshikawa, *J. Am. Chem. Soc.* 125 (2003) 4414.
- [7] V. A. Bloomfield, *Biopolymers* 44, (1997) 269.
- [8] V. Y. Borue and I. Y. Erukhimovich, *Macromolecules* 23 (1990) 3625.
- [9] M. Castelnovo and J.-F. Joanny, *Eur. Phys. J. E* 6 (2001) 377.
- [10] M. Olvera de la Cruz, L. Belloni, M. Delsanti, J. P. Dalbiez, O. Spalla and M. Drifford, *J. Chem. Phys.* 103 (1995) 5781.
- [11] E. Raspaud, M. Olvera de la Cruz, J. -L. Sikorav, and F. Livolant, *Biophys. J.* 74 (1998) 381.
- [12] T. T. Nguyen, I. Rouzina, and B. I. Shklovskii, *J. Chem. Phys.* 112 (2000) 2562.
- [13] T. T. Nguyen and B. I. Shklovskii, *J. Chem. Phys.* 115 (2001) 7298.
- [14] R. Zhang and B. I. Shklovskii, *Phys. Rev. E* 69 (2004) 021909.
- [15] R. Zhang and B. I. Shklovskii, *Physica A* 352 (2005) 216.
- [16] L. D. Landau and E. M. Lifshitz, *Statistical Physics, Part 1* 3rd ed. (Butterworth-Heinemann, Oxford, 1980).
- [17] T. T. Nguyen and B. I. Shklovskii, *Phys. Rev. Lett.* 89 (2002) 018101.
- [18] In this paper, for simplicity, we do not discriminate between the size of the monomer and the distance between charges in the polymer. This is a reasonable approximation for strongly charged polyelectrolytes ($b \simeq l_B = 7\text{\AA}$).
- [19] R. Zhang and B. I. Shklovskii, cond-mat/0310321.
- [20] T. T. Nguyen and B. I. Shklovskii, *Phys. Rev. E* 65 (2002) 031409.
- [21] B.-Y. Ha, and A. J. Liu, *Europhys. Lett.* 46 (1999) 624.